

9-9-1987

## Developments in Voltage Contrast

P. Girard

*Université des Sciences et Techniques du Languedoc*

Follow this and additional works at: <https://digitalcommons.usu.edu/microscopy>



Part of the [Biology Commons](#)

---

### Recommended Citation

Girard, P. (1987) "Developments in Voltage Contrast," *Scanning Microscopy*. Vol. 2 : No. 1 , Article 15.  
Available at: <https://digitalcommons.usu.edu/microscopy/vol2/iss1/15>

This Article is brought to you for free and open access by the Western Dairy Center at DigitalCommons@USU. It has been accepted for inclusion in Scanning Microscopy by an authorized administrator of DigitalCommons@USU. For more information, please contact [digitalcommons@usu.edu](mailto:digitalcommons@usu.edu).



DEVELOPMENTS IN VOLTAGE CONTRAST

P. Girard

Laboratoire d'Automatique et de Microélectronique de Montpellier,  
U.S.T.L. Place Eugène Bataillon, 34060 Montpellier cedex, France

(Received for publication February 05, 1987, and in revised form September 09, 1987)

Abstract

The aim of this paper is to give a review of the main steps that have led to voltage contrast equipment available to day for integrated circuit testing.

The main parameters related to quantitative voltage evaluations are discussed in the case of measurements on integrated circuits metal stripes as well as on buried lines. They concern : the reduction of the local field effects, the voltage resolution improvements on the energy analysers, and the time resolution. Results concerning the E-beam perturbation of MOS circuits are reported. Due to the test conditions and the presence of additional elements inside the microscope column limitations are introduced in spatial resolution. The performances available are given. They are consistent with today's microelectronics. But, for the future, we show in this paper that the debate is not closed. It concerns both basic improvements and developments related to the use of the E-beam testers.

Introduction

The principle of voltage contrast has been known for a long time (44) but only this last year's equipment based on this technique is commercially available. This is the result of two factors : i) the increased needs in fault diagnosis in integrated circuits (IC), where the element sizes are reducing, ii) the parallel improvements in electron beam equipment resulting from advances in basic and applied research.

The purpose of this paper is to give a review of the different problems that must be solved in order to provide characteristics adapted to microelectronics. First, we shall give an outline of the voltage contrast principle. Secondly, we shall detail the significant characteristics of the system, i.e., the voltage, time and spatial resolutions that both depend on spectrometer and microscope working conditions. Finally, we shall deal with the new developments that lead to systems which can be used by non-specialists, for example in a design work station. In the different steps, we shall remember that there is always work for researchers essentially due to future microelectronics needs.

Voltage Contrast

Principle

In electron microscopy any phenomenon creating a variation in the number of collected electrons by the detector gives rise to a contrast. Among the reemitted electrons, different energies can be found : i) the backscattered electrons with  $E_b \approx 0.7 E_p$ , ii) the secondary electrons (SE) where the energy is by definition limited to 50 eV.

The contrasts mainly related to backscattered electrons are the atomic and the crystalline contrasts. The topographic, magnetic, and voltage contrasts essentially concern the secondaries, and arise from low penetration zones. Our field of interest, the voltage contrast, needs to be consequently intensified in opposition to the other cases.

The energy distribution of secondary electrons  $N(E)$  has been extensively studied by Kollath (29), and can be written at first approximation :

KEY WORDS : Voltage contrast, Integrated circuits testing, Spatial resolution, Waveform measurements, Electron beam damages, Metal Oxide Semiconductor Transistors, Reconfiguration.

Address for correspondence :

P. Girard, Laboratoire d'Automatique et de Microélectronique de Montpellier, Université des Sciences et Techniques du Languedoc, Place Eugène Bataillon - 34060 MONTPELLIER cedex, France  
Phone No. (33) 67 63 41 84

$$N(E_0) = 1.5 E_0 \exp ( 2 - (8/3 E_0)^{1/2} ) \quad (1)$$

This function peaks at about 2 eV, and is eventually shifted by the target polarisation  $V_t$  by the amount  $-qV_t$ . This shift is the basis of quantitative voltage evaluation.

Assuming for example a two dimensional geometry for the detection system, the detected current becomes :

$$I_{det} = I_{sat} \int_{-\frac{\pi}{2}}^{+\frac{\pi}{2}} \left[ \begin{array}{l} E_{max} \\ C(\theta) N(E_0) F(E_0) d\theta dE_0 \\ E_{min} \end{array} \right] \quad (2)$$

where :

-  $\theta$  represents the angle of emission with respect to the normal to the specimen,

-  $C(\theta)$  represents the collection coefficient for the detection system. The transmission coefficient  $T$  of the energy analyser is implicitly included.

-  $F(E_0)$  represents an eventual filtering function inside the detection system depending on the secondary energy.

This simple presentation of the phenomenon assumes a stabilization of the emission coefficient during the measurements. Consequently, charging effects occurring in insulators, or insulated metal pads, and contamination cases are excluded. Besides changes in the topography or nature of the material are obviously ruled out.

In the ideal case : i)  $F(E_0)$  is a step function, i.e.,  $F(E_0) = 1$  only if  $E \geq E_1$ , ii)  $C(\theta)$  is poorly sensitive to neighbouring electrical conditions. Assuming now a target polarisation, the relation (2) is simplified :

$$I_{det} = I_{sat} \int_{-\frac{\pi}{2}}^{+\frac{\pi}{2}} \left[ \begin{array}{l} 50 \text{ eV} \\ C(\theta) N(E + qV_t) d\theta dE \\ E_1 \end{array} \right] \quad (3)$$

and the detected current becomes a non-linear but monotonic function of the specimen voltage (fig. 1). The minimum and maximum energies,  $E_{min}$  and  $E_{max}$ , are supposed to be respectively 0 and 50 eV. In order to get quantitative voltage evaluations, the energy  $E_1$  can be automatically adjusted in order to give a constant signal (8, 9) and when  $E_1 = E_{10} - qV_t$  with an  $E_{10}$  value roughly located in the 0 - 5 eV range it is obtained whatever  $V_t$  might be.

Consequently, quantitative evaluations of local potentials can be achieved on metal test pads with great dimensions and only differential measurements (43,1) are valuable in general. In other words at a given point a signal changing with time is now correctly evaluated, but a comparison of absolute values is difficult due to the possible local secondary emission variations. This point is fundamental with a voltage contrast quantitative approach.

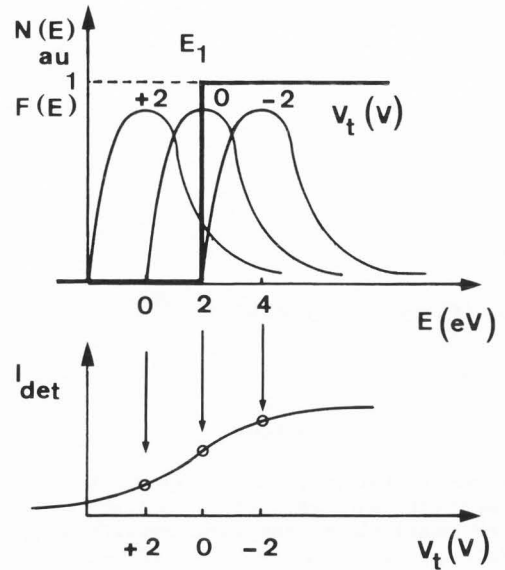


Fig. 1 : Sketch of the detected current as a function of the target voltage. They correspond to the areas at the right hand side of the limit  $E_1$ .

Evaluation of quantitative voltage on IC metal stripes

The accuracy in voltage measurements supposes: i) the right amplitude evaluation depending on voltage resolution and voltage errors introduced by the electrical environment around the tested point ; ii) a time resolution consistent with the investigated signal periods.

The voltage resolution depends on the noise sources in all the detection chain. The three main terms concern the primary beam, the secondary yield and the influence of backscattered electrons (38). The backscattered can act directly or indirectly via secondaries generated inside the spectrometer.

Assuming shot noise sources, and taking into account the two first elements, the minimum estimated voltage which can be detected in the closed loop mode is (19) :

$$\Delta V_{min} = n \sqrt{\Delta f / I_p} C \quad (4)$$

On the one hand, it depends on the admitted signal over noise ratio  $n \approx 3$ , the bandwidth  $\Delta f$  for the detection system, and the primary beam current  $I_p$ . If we write the spot diameter in its simplest form (see rel. 8), say  $d^2 \propto I_p / B$  it comes :

$$\Delta V_{min} = n \sqrt{\Delta f / B} \quad 1/d \quad (5)$$

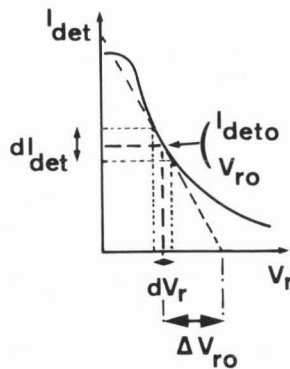
and in some cases a compromise is required between voltage and spatial resolution.

On the other hand, the constant  $C$  may be split in two terms. The first term  $2q(1 + \delta) / \delta$  depends on the secondary electron yield  $\delta$ .

The second term is related to the spectrometer characteristics, i.e.:

$$(1/\sqrt{T}) \cdot (I_{det} / ((dI_{det}/dV_r))) = \Delta V_{ro} / \sqrt{T} \quad (6)$$

Fig. 2 : Detected secondary electrons current versus the retarding voltage  $V_r$ . The working point coordinates are :  $V_{ro}$  and  $I_{deto}$ .



The different elements are defined on Fig. 2 and spectrometer sketch on Fig. 3.

It is clear that the voltage resolution depends on the transmission  $T$  of the spectrometer and the optimization of the working point. Taking into account the secondary emission spectrum for aluminium and realistic parameters, this model predicts a maximum attainable resolution of 0.08 mV. As mentioned by the authors (38), the experimental value lies around 0.5 mV on large test pads. The main reason originates probably in the influence of the backscattered electrons not taken into account here.

Let us now come back to the relations (2) and (3). On the one hand, when the filtering function  $F(E)$  for the energy analyser approaches the ideal step case, the detected secondary emission integral spectrum does the same. On the other hand, the insensitivity of  $C(\theta)$  to IC electrical and measurement conditions gives a stable voltage resolution. In other words, the conservation of shape and amplitude of the S curves need to be approached for good accuracy voltage measurements.

To satisfy this requirement the major problem is the elimination of the local field or microfields effect. To give an order of magnitude for a 0-5 V logic IC, a 2.5  $\mu\text{m}$  space between two adjacent lines gives a 2 kV/mm electrical field at the specimen surface. Due to the fact that technology is improving higher and higher local fields will appear in the future.

The combination between the voltage at the measured point and neighbouring ones gives rise (11,41) : i) to recapture some of the secondary electrons by the specimen, ii) to changes in the mean angle of secondary electron emission.

This effect is responsible for voltage contrast imaging obtained in classical SEMs without any energy analysers. In the case of quantitative voltage contrast this parasitic effect is responsible for: i) cross talking, i.e., the voltage of the adjacent lines is partly read on the measured element, ii) changes in electron trajectories outside and inside the spectrometer. Consequently both  $C(\theta)$  and  $F(E)$  are affected. It concerns image mode operation as well as quantitative voltage evaluations.

In order to reduce these effects with respect to the SE energy shifts, it has been proposed to apply a strong voltage between the sample and an

extraction grid. The vertical fields then obtained have the same order of magnitude we mentioned previously, so on the one hand the collection is improved. But on the other hand it induces a parasitic charge on insulator zones then causing problems in examination of buried lines (22). The elimination of the lowest energetic electrons, i.e., the most sensitive to microfields also constitutes an improvement (8).

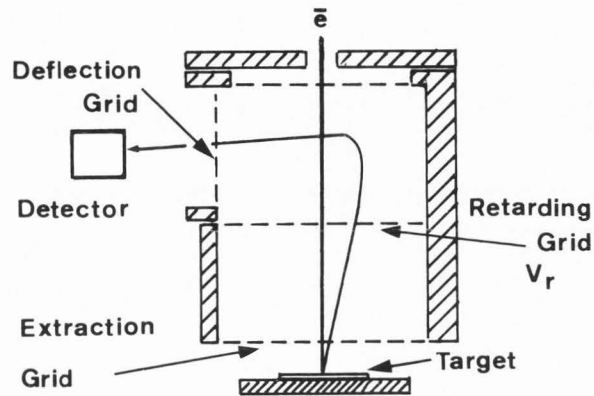


Fig. 3 : Example of a planar retarding field spectrometer (below the lens type) after ref 8.

Different types of energy analysers have been developed, Plows (45) pioneered in this domain, and was followed by many groups. Feuerbaum then developed a planar analyser (8). The principle of the system is the following (fig. 3) : the analyzer is placed under the objective lens of a conventional SEM, the electrons are first accelerated in the extraction field, decelerated in the retarding field and then deflected towards the SE detector. The high pass filter function  $F(E)$  is then obtained with  $E_1 = -qV_r$ , where  $V_r$  is the retarding grid potential. Only the electrons having an energy superior to this value are able to reach the detector. Then the constant signal condition corresponds to  $\Delta V_t = \Delta V_r$ .

However it must be noticed that the filtering function is not perfect with the planar analyser. It arises from the fact that the kinetic energy considered by the retarding potential concerns only the part of the velocity vector normal to the grid. Concerning this point, the superiority of hemispherical analyser is obvious (23).

The angular distribution of reemitted secondaries can be either a normal process or related to the microfield or topographic effects. In the planar case, it decreases the sensitivity of the detection by lowering the transmitted number of electrons even with a convenient energy but with a bad angle. This effect decreases with electron refocussing using long analysers in the lens (39). In other terms, the sharpness of the  $F(E)$  function has been increased and the  $C(\theta)$  sensitivity to initial angular distribution decreased. Then spectrometer coefficients  $C$  (see rel. 4) values of 6 - 8. 10<sup>-9</sup> (Volt .  $\sqrt{\text{As}}$ ) have been reported.

But nowadays the debate is not closed and for example, magnetic focussing analysers using a magnetic lens below the specimen are under study

(14). Very interesting results concerning spatial resolution, microfield effects, with low extraction fields have been announced.

The time resolution is conditioned by the sampling times, the magnitude and stability of the delays occurring between the initial synchronization signal and the final element in the detection chain. In the case of real time operation, the high frequency limitation is given by the linearization feedback loop to about 0.5 MHz. On the opposite for stroboscopic modes, assuming fixed delays, the time resolution depends on the sampling times. The resolution due to video signal gating is limited to around 50 ns (5) but it is greatly improved in the case of beam blanking operations.

The chopping systems concern mainly travelling wave structures (19), reentrant cavities (51) and plate capacitors (1,44). Since general purpose equipment are generally required, the best flexibility is given by the capacitor system. It concerns energies, primary beam currents and driving frequency (36).

The blanker is generally situated around the upper lens of the microscope near the gun. The electrostatic deflection angle  $\alpha(f)$  is frequency dependent. The beam chopper can be either a real aperture or a knife edge, or the image of the final aperture near the objective lens.

The angular deviation writes (32) :

$$\tan \alpha(f) \approx \alpha(f) = \alpha_{\max} \sin(\pi f L / v) / (\pi f L / v) \quad (7)$$

$$\text{with} \quad \alpha_{\max} = (V_{de} / V) (L / 2d_0)$$

$V_{de}$  and  $qV$  correspond respectively to the applied voltage to the capacitor plates and the primary electrons energy. They have a velocity  $v$ .  $L$  represents the length of the plates to be travelled by the electrons and do their spacing.

The first zero value corresponds to a transit time equal to 270 ps with  $V = 1$  kV and  $L = 0.5$  cm. In order to overcome this time limitation, it has been proposed to increase the blanker sensitivity. Consequently a suitable beam deviation can be obtained with a low  $V_{de}$  variation and then a possible duration much lower than the voltage driving period  $1/f$  is achievable.

This way assumes the optimization of the blanker position inside the column (17,18) and its design. It also provides reduction in spot size blanking degradations. They are produced by i) crossover motions during deflection rise and decay times (44), an ellipticity is introduced in the spot shape, ii) increasing in the electron energy spread (33). In this case the chromatic aberration term in rel. (8) is changed.

On prototypes blanking times of 80 and 10 ps have been obtained. They use respectively a double plate system (24) or a single plate associated with a supplementary lens (36).

But the exploration of this field is not closed. The time of flight of the electrons between target and detector is specimen voltage dependent. The jitter introduced needs to be taken

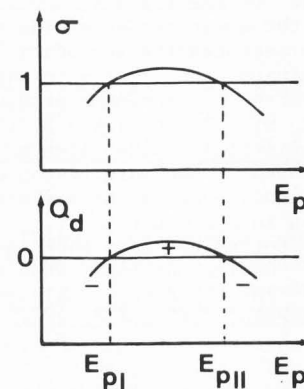
into account for time voltage variations lying in these magnitudes (13). To our knowledge, 100 ps corresponds to the results obtained in today's normally available E-beam testers.

#### A way in progress : measurements on buried lines

Since real ICs are generally covered with a passivation layer, nowadays the voltage evaluation on buried lines is an essential problem. Research on the field has been extensively developed these recent years (11,21,52).

Because of the MOS circuits sensitivity to electron beam irradiations, we will see that later, the creation of a conductive channel between the surface and the buried line is no longer suitable. The only suitable way uses the capacitive coupling between the buried conductor and a charged surface sheet. This is called the capacitive coupling voltage contrast (CCVC).

Fig. 4 : Sketch of the ratio  $\sigma$  between the number of reemitted and incident numbers of electrons versus the primary electrons energy  $E_p$ . The deposited charge  $Q_d$  is also indicated. The existence of  $\sigma > 1$  is a necessary precondition for CCVC.



All the difficulty lies in the creation of a stable charged surface sheet with E-beam scanning. It results from the fact that the ratio between the number of reemitted and incident electrons is energy dependent as sketched on Fig.4. The N shaped variation presents a maxima generally superior to  $\sigma = 1$ , the energies  $E_{pI}$  and  $E_{pII}$  correspond to  $\sigma = 1$ . Inside this range, the deposited charge has a positive sign, outside it is negative. Concerning  $\text{SiO}_2$ ,  $E_{pII}$  merges inside the 1 - 2.5 keV range (2,22,54), this value is consequently opened to classical SEMs. However good stability charges correspond to : i) initial primary energies  $E_{p0} < E_{pII}$ , ii) extraction fields lower than 100 V/mm.

The physical process of charge deposition can be explained as follows (22) : the surface first begins to be positively charged, its potential  $\phi$  increases. The secondary electrons can no longer leave the surface. Then  $\sigma$  and the rate of charging are decreased. This process is going on until, in the simplest case, a balance between incident and reemitted currents is reached. The primary electrons energy seen by the surface remains unchanged and the surface potential  $\phi$  stays at first approximation in the 0,+10 V range.

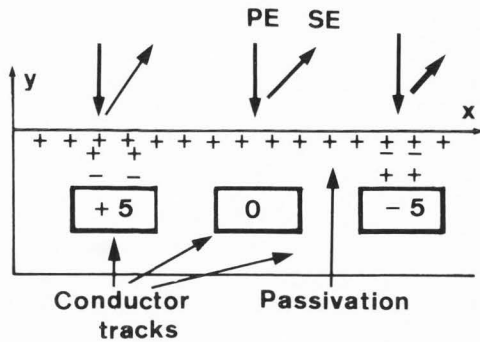


Fig. 5 : Model for CCVC (22). Schematic view of the charges configuration in three different cases. They correspond to the switching on time at the indicated voltages. Instantaneously reemitted SE currents are also indicated.

Once the surface has been charged, if for example, the buried line voltage changes from 0 to + 5 volts (see Fig. 5), the surface voltage is locally increased. A supplementary barrier appears above the track and the secondary emitted current readily decreases. The balance resulting from the first charging process is destroyed until the supplementary induced charge  $Q = \Delta Vt/C_{pass}$  is cancelled by the absorbed current,  $C_{pass}$  represents the passivation layer capacitance. The corresponding storage time  $T_s$  is the second fundamental parameter for CCVC, the first being  $E_{po}$ .

This period  $T_s$  decreases with : i) the current density falling on the sample, ii) the passivation thickness, iii) the difference  $E_{po} - E_{pII}$ .

It is clear that the conditions of quantitative voltage evaluations are approached when the buried target voltage period  $T_t$  is much lower than the storage period  $T_s$  (Fig. 6).

Consequently, turning on and off DC and AC voltages can be detected with essentially low current densities corresponding to large scanned areas, i.e.  $\approx 1 \text{ mm}^2$ . This method is well adapted for semiquantitative image modes such as voltage coding (55), frequency tracing (3), etc.

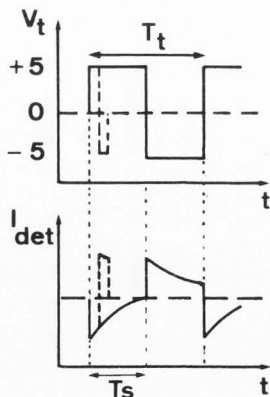


Fig. 6 : Diagram showing the correspondence between the buried line voltage and the SE currents versus time t. Two signal periods are shown.

With a spectrometer the quantitative determination of voltages, i.e. the waveform mode, remains a little bit more difficult due to the fact the beam is permanently positioned at the same place. The stroboscopic mode is generally achievable.

Assuming : i) no drastic current probe limitations, ii) a suitable capacitive coupling with the track considered, iii) no special signal losses due to electron irradiation, the preceding voltage and time resolutions seen on conductor pads remain on the whole valid. The spatial resolution could eventually be degraded on the edges of the tracks.

Conditions for Electron-Beam testing

The conditions concerning electron-beam testing arise from two types of considerations : i) the perturbation of integrated circuits by the beam must be avoided, ii) the results need to be as significant as possible with respect to the electrical state of the examined point. This last fact will be simply mentioned in this section and is related to spatial resolution.

The non-perturbation conditions are related to: first the interaction of the beam with sensitive parts of the devices and secondly to impressed currents on the IC.

Radiation like type damages

The electrons impinging on a semiconductor or more generally an insulator in integrated circuits give rise to the following phenomenon : the primary electrons circulate inside the material, the interaction zone has a pear-like form where electron hole pairs are created, then these carriers diffuse outside and finally recombine. It results first in a possibility of radiation type damage and secondly short circuiting possibilities. The latter effect has, at first sight, some importance essentially in devices where possible current sources have finite possibilities, for example, like in Famos (10), where the charge located in a floating gate may be evacuated. Generally, in E-beam testing conditions with low beam energies, the electron penetration is insufficient in order to produce such effects. The interaction zone has been estimated, at first approximation, by a sphere with a diameter  $D$  with  $D \propto E_p^{5/3} (\rho Z)^{-1}$  following the Kanaya semiempirical model (28). The primary energy, cubic mass and atomic number are respectively represented by  $E_p$ ,  $\rho$  and  $Z$ , typically when changing the energy from 1 to 5 keV the sphere diameter increases from 0.03  $\mu\text{m}$  to 0.45  $\mu\text{m}$ .

Results concerning the influence of low energy E-beam on MOS transistors have been reported in the literature (15,20,40,42). It has been observed : i) a negative threshold voltage shift in the 1-18 keV energy range, ii) generally a linear relationship between the magnitude of the shift and the incident dose falling on the device  $D = I_p \cdot t / S$  where  $t$  and  $S$  represent the irradiation time and the scanned area. From our results, the shifts are independent of the channel type and dimensions of the transistor (Fig.7). However other authors mentioned an increasing of the effect at the shortest channels (40) i.e. lower than 3 micrometers, these differences could be related to the technology. The magnitudes observed

are independent of device polarization or irradiation mode (DC or 2ns chopping time).

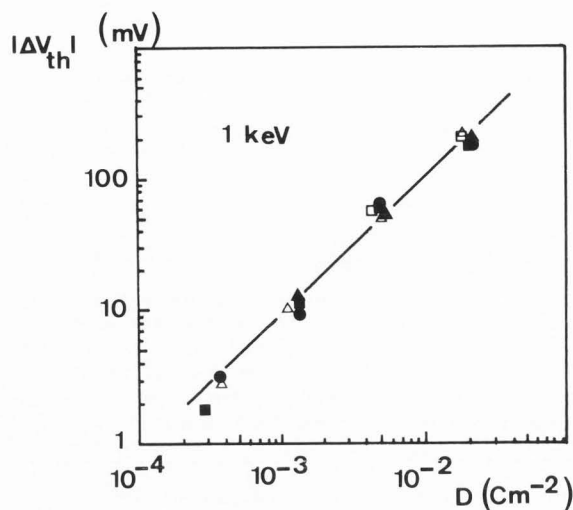


Fig. 7 : 1 keV threshold voltages shifts. Types of transistors examined : i) W/Z = 50/50, n channel (■), p channel (□), ii) W/Z = 100/3 n (▲) , p (△), iii) W/Z = 3/25 ,n (●). The dimensions correspond to micrometers.

The three possible physical effects for MOS perturbations are (25) : i) direct charging, ii) trap creation inside the gate oxide, iii) indirect charging of normally existing flaws. Our experiments have been achieved with all the electrodes grounded, the threshold shifts have always the same sign within the 1-6 keV range, then the first possibility is ruled out. The penetration of the 600 Å gate oxide across 8000 Å SiO<sub>2</sub> plus 5000 Å polysilicium is unlikely. The only possible reason concerns the charging of flaws by reemitted X photons from the top oxide.

The sensitivity depends drastically on the primary energy E<sub>p</sub> as we can see on our results (fig.8). In the highest energy range, i.e. 5 to 18 keV, other authors (42) have evaluated the fraction f<sub>d</sub> of the primary energy deposited in the gate oxide. This term decreases from some 10<sup>-2</sup> when the gate oxide is reached by the electrons down to 10<sup>-6</sup> at 5 keV. In this last case, the primary particles remain reasonably localized outside the gate oxide. Simulations taking into account characteristic SiO<sub>2</sub> photons showed a right order of magnitude for the 5-8 keV f<sub>d</sub>.

In fig. 8 we report the possible irradiation times versus the primary energies, these times correspond to 0.1 volt threshold shifts. The normal values are situated between -1 and + 1 volt owing to different transistor types. The non-perturbing conditions depend also on the magnification conditions.

If we adopt a 1 nA mean beam current and 1 keV at x 100 linear magnification corresponding to a 1 x 0.8 mm<sup>2</sup> field, the exposure time exceeds 20 h so no damage is obviously expected. But if a 100 x 80 μm<sup>2</sup> field is required, the experimentalist has only 10 minutes of safe working condi-

tions. These previous times are considerably reduced typically by a factor 20 and 200 at 2 and 5 keV, respectively.

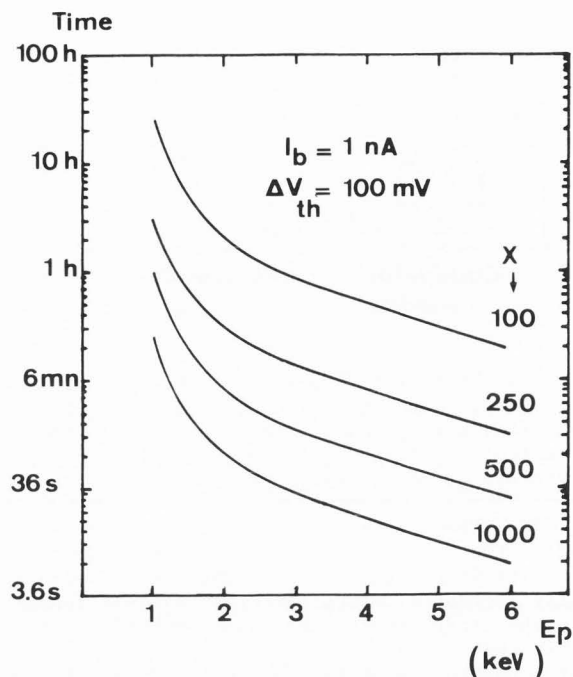


Fig. 8 : Diagram showing the expected exposure times at E-Beam currents versus primary energies. The threshold voltage shift and the mean beam current are respectively 0.1 Volt and 1nA. The different curves have the linear magnification as parameter.

#### Impressed currents

Previously we have seen that the absorbed current due to an incident electron beam I<sub>p</sub> is I<sub>a</sub> = (σ - 1) I<sub>p</sub>.

The non zero charge can alter the observation or the device working conditions, for example, if charge evacuation is weak. In this case breakdown conditions can also occur in the most drastic conditions (49). In other cases (35), aluminium nodes in IC (30) or oxide encapsulated floating gate MOS have been activated with the E-beam (46). This positive use of impressed charges contributes to E-beam switches achievements. This promising subject will be examined in the last part of this paper.

Briefly stated, except for special devices, the non-charging conditions are less restrictive than the radiation damage ones. The E-beam testing energies started from 2.5 keV (55) down to 0.7 keV (31). Consequently the energies currently available in EBT equipment are now around 1 KeV and remains consistent with today's IC technology.

#### Spatial resolution, related problems : Image mode

The spatial resolution is a crucial problem with E-beam testing, because quantitative modes of operation as well as qualitative ones are affected. Due to the fact that low primary energies and

## Developments in Voltage Contrast

secondaries are concerned, the main point is the spot diameter.

The image quality remains conditioned by the spot size and it is currently admitted that this size must not exceed 1/5 of the picture element to be visualized (4). In the quantitative voltage evaluation, the diameter needs to be smaller than the aluminium stripe width. In the opposite large metal test pads are required.

In order to clarify these ideas, the SEM conditions of operation are the following :

i) 1 keV primary beam energy in order to avoid IC disturbances, ii) about 1 nA DC beam current. In this last case operation in stroboscopic mode at 1 ns gives only 6 incident electrons per pulse. In order to have suitable signal to noise ratio and measurement durations, it is not recommended to decrease this value. Concerning classical sources SEMs, i.e., for tungsten or lanthanum hexaboride sources, the square value of the spot diameter  $d$  is equal to the sum of the square values of the error terms (16,53) :

$$d^2 = (4 I_p / \pi^2 B + (1.22 \lambda)^2) 1/\alpha^2 + 1/4 C_s^2 \alpha^6 + C_c^2 (\Delta E_p / E_p)^2 \alpha^2 \quad (8)$$

It depends on the characteristics concerning:

- the gun via its brightness  $B$ , the beam current  $I_p$ , the associated wavelength  $\lambda$ , the relative energetic dispersion  $\Delta E_p / E_p$ ,

- the objective lens with its chromatic and spherical aberration terms, respectively,  $C_c$  and  $C_s$ ,

- the conditions of observation via the half beam aperture  $\alpha = da/(2 wd)$  where  $da$  and  $wd$  represent, respectively, the aperture of the beam at objective lens and the working distance.

To give an idea of the behavior, at first approximation the diffraction term can readily be ruled out and, at the highest currents, if we neglect the aberrations related to the objective:

$$d = 2/\pi (I_p/B)^{1/2} 1/\alpha \propto (I_p/V)^{1/2} wd \quad (9)$$

First, it is interesting to note that the spot size is an increasing function of the working distance, from our experiments the measurements give exponents between 1/2 to 1. As we work in the worst conditions to obtain good images, i.e., with essentially low energies and high currents, it is interesting to use a short working distance spectrometer.

Secondly, the higher the brightness the best the results will be. Gun choices oscillate between tungsten and lanthanum hexaboride, there is no general clear evidence to use one precise type. New ways seem to be either multi-electrode low voltage guns or, in the future, field effects guns.

Thirdly, it has been mentioned that low blanking times can affect spatial resolution. However, under optimized conditions, stigmator corrections are effective and an increase of a factor 2 at the lower blanking time seems reasonably expected.

Consequently, the spatial resolution remains a satisfactory compromise between these different points and each microscope coupled with a blanker

and analyzer requires a specific solution.

In order to accurately determine the order of magnitude we can say that at 1 keV, 1 nA DC current, chopped mode (2 ns), the knife edge method results (27) give now currently 0.3 micrometer spot size.

### Recent developments and future prospects

#### Functions available

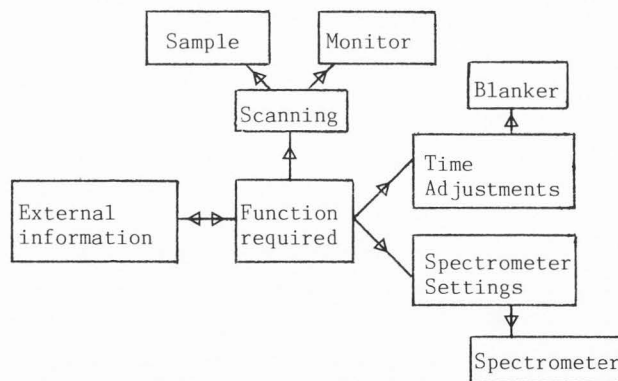
Due to the developments concerning the EBT equipment in the 80's the function  $V(x,y,t)$  is normally attainable on metal nodes or less currently on buried stripes (12,22) with some picture or analog signal processing. The field of view normally admitted is about  $200 \times 300 \mu m^2$  and a controlled stage displacement is generally required.

The possibilities (55) are summarized in Table 1. with the techniques associated.

Table 1 . Functions generally achieved on voltage contrast systems.

IMAGE MODE	WAVEFORM MODE
1) $V(x,y,t)$	$V(x_j, y_j, t)$
<ul style="list-style-type: none"> <li>i) Static or low frequency circuit operation. Possible signal processing techniques (5).</li> <li>ii) High frequencies (blanker required) : Stroboscopic mode.</li> </ul>	<ul style="list-style-type: none"> <li>Sampling techniques : multi waveform measurements.</li> <li>Logic thresholds : logic state mapping.</li> <li>Frequency mappings (3).</li> </ul>
2) $V(x,t)$	Voltage coding (34).

Table 2 : Functional organization of equipment devoted to E-beam testing of ICs.



The suitable conditions for equipment operation require the coordination of the different hardware functions and information input-outputs as shown in Table 2 (55,37). A computer controlled system is obviously required in order to achieve a good efficiency and some comfort in working conditions.

New developments

This type of equipment can be typically used in IC testing sequences corresponding first to fault detection and secondly to fault diagnosis, this latter step is really in the field of the EBT systems.

Fault detection is normally achieved with input-output testers with high speed conditions of operation available today. They are dependent on the various electrical inputs of the circuits, in the future the number of available conditions could be increased using E-beam observable nodes. The test vectors concerning the faulty operations could consequently be extracted.

Fault analysis with the EBT gives the location and the possible electrical reason for the defect. Typical processes have yet to be given (7), the picture electrical behavior gives first the geographical faulty zone location and secondly waveform measurements provide additional information. Essentially due to the fact that: i) the number of elements implemented per unit surface, ii) the test pattern complexity increasing, an automated procedure remains the only efficient way. Finally such equipment might be put in the hands of design engineers (6).

First a convenient element for comparison is needed. In failure analysis, for example, it is possible to refer to the electrical diagrams, in production a good device may be a solution. Concerning the design verification, a layout simulation remains the best way. Some attempts have been recently stated in the literature (48) with semi-custom circuits (ASICs). A link has been established between the circuit description and the layout data and consequently a biunique relation exists between the input test pattern and the simulated logical states picture.

Secondly the matching between this picture and the image extracted from the SEM is obtained. Due to the large number of operations required, a host computer is used. Then, once the faulty zone is obtained, waveforms on sensitive nodes give further information. Now it opens the way to automatic defect recognition via expert systems.

The preceding ways only concern the use of the electron beam as a passive probe. The active function of this probe has been reported in the case of experimental self test circuits (50) or memories (46). The activation of switches with the electrons could constitute progress, for example in : i) testing with the possibility of blocs partitioning, ii) reconfiguration in order to provide easy testing or yield improvements in zero defect devices. This high possibility of testing and recovery of defects is given by the same instrument, the SEM. Among the different possibilities investigated, the charging of floating gate transistors causing a threshold voltage shift is the most promising one (15,46). Consequently microscope columns giving the possibility to work at three primary energies with optimized image shifts would be sufficient. The energies range is limited between 5 keV for reconfiguration and 1 keV for testing.

Conclusion

The voltage contrast techniques is now coming of adult age (26,47). This fact has been obtained with progress in basic and applied research concerning mainly the electron detectors and the test methods. Practically it results from a compromise between the conditions of non-destructive testing, the spatial, time and voltage resolution. EBT systems are also well serviced by convenient software procedures.

The applications field of the EBT equipment is wide. It concerns reliability studies in production as well as in failure analysis. The major developments are certainly devoted to the design and test of complex integrated circuits where new ways are opened with the future active function of the electron probe.

Acknowledgements

We gratefully acknowledge the European Communities who supported a part of this work with the ESPRIT 824 program.

References

- 1- Balk LJ, Feuerbaum HP, Kubalek E, Menzel E (1976) Quantitative voltage contrast at high frequencies in the SEM. Scanning Electron Microsc. 1976 ; I : 615-624.
- 2- Brunner M, Menzel E (1983) Surface potential measurements on floating targets with a parallel beam technique. J.Vac.Sci.Techn. B1(4), 1344-1348.
- 3- Brust HD, Fox F (1985) Logic state tracing : electron beam testing by correlation. Microelectronic Engineering 3, 191-202, North Holland ed.
- 4- Cocito M, Soldani D (1983) Evaluation of the performance of an electron beam testing system based on commercially available subsystems. Scanning Electron Microsc. 1983 ; I : 45-54.
- 5- Collin JP, Viacroze T (1985) E-beam testing : image and signal processing for the failure analysis of VLSI components. Proceedings of International Symposium on Techniques of Failure Analysis, Los Angeles, 89-97, Atfa ed. Torrance CAL 90510 USA.
- 6- Concina S, Liu G, Lattanzi L, Reyfman S, Richardson N (1986) Software integration in a workstation based E-beam tester. Proceedings Int. Test Conf., Washington, 1986, pp. 644-649, IEEE Series Press, Washington DC.
- 7- Crichton G, Fazekas P, Wolfgang E (1980) Electron beam testing of microprocessors. IEEE Test Conference, 1980, 444-449.
- 8- Feuerbaum HP (1979) VLSI testing using the electron probe, Scanning Electron Microsc. 1979 ; I : 285-296.
- 9- Flemming JP, Ward EW (1970) A technique for accurate measurement using a retarding field analyser in the scanning electron microscopy. Scanning Electron Microsc. 1970 : 465-470.
- 10- Frohman Bentchkovsky D (1974) Famos - A new semiconductor charge storage device. Solid State Electronics 17, 517-529.

## Developments in Voltage Contrast

- 11- Fujioka H, Nakamae K, Ura K (1981) Local field effects on voltage measurement using a retarding field analyser. *Scanning Electron Microsc.* ; 1981; I: 323-332.
- 12- Fujioka H, Nakamae K, Ura K (1983) Voltage measurements on passivated electrodes with the scanning electron microscope. *Scanning Electron Microsc.* 1983 ; III : 1157-1162.
- 13- Fujioka H, Nakamae K, Ura K (1986) Analysis of transit time effect on the stroboscopic voltage contrast in scanning electron microscope. *J. Phys. D : Appl. Phys.* 18, 1019-1027.
- 14- Garth SCJ, Nixon WC, Spicer DF (1986) Magnetic field extraction of secondary electron for accurate integrated circuit voltage measurement. *J. of Vac. Sci. Techn. B(4)*, 1, 217-220, Jan-Feb.
- 15- Girard P, Roche FM, Pistoulet B (1986) Electron beam effects on VLSI MOS. Conditions for testing and reconfiguration. *Wafer Scale Integration*. 301-310. G.Saucier, J.Trilhe (eds), Elsevier Science Publishers BV (North Holland) IFIP.
- 16- Goldstein JL, Yakowitz H (1975) *Practical scanning electron microscopy*. Plenum Press, New York, London.
- 17- Gopinath A, Hill MS (1974), Some aspects of the stroboscopic mode : a review. *Scanning Electron Microsc.* 1974: 235-242.
- 18- Gopinath A, Hill MS (1977) Deflection beam chopping in the SEM. *Journal of Physics E, Scient. Instr.* 10, 229-236.
- 19- Gopinath A (1977) Estimate of minimum measurable in the SEM. *J. of Phys. E.10*, 911-913.
- 20- Görlich S, Kubalek E (1985) Electron beam induced damage on passivated MOS. *Scanning Electron Microsc.* 1985 ; I : 81-95.
- 21- Görlich G (1986) Electron beam testing of passivated integrated MOS circuits. Thesis, University of Duisburg 1986.
- 22- Görlich S, Herrmann KD, Reiners W, Kubalek E (1986) Capacitive coupling voltage contrast, *Scanning Electron Microsc.* 1986; II: 447-464.
- 23- Goto H, Ito A, Furukawa Y, Inagaki T (1981) Hemispherical retarding type energy analyser for I.C. testing by electron beam. *J. Vac. Sci. Tech.*, 4, 19(4), 1030-1032, Nov. Dec.
- 24- Goto H, Ozaki K, Ishizuka T, Ito A, Furukawa H, Inagaki T (1984) Electron beam prober for LSI testing with 100 ps time resolution. *International Test Conference*, Oct. 1st-3rd, 1984, 543-549, IEEE Computer Society Philadelphia Section ed.
- 25- Holmes-Siedle AG, Zaininger KA (1968) The physics of failure of MIS devices under irradiation. *IEEE Trans. on reliability*, R17, 1, 34-44, March 1968.
- 26- Iscoff R (1985) E Beam probing systems : filling the submicron gap. *Semiconductor International*, 62-68.
- 27- Joy DC (1974) SEM parameters and their measurements. *Scanning Electron Microsc.* 1974 : 327-334.
- 28- Kanaya K, Okayama S (1972) Penetration and energy loss theory of electrons in solid targets. *J. Phys. D, Appl. Phys.* Vol. 5, 43-58.
- 29- Kollath R (1956) *Handbuch der Physik*, Vol 21, 241. (Springer Verlag Germany).
- 30- Könemann B, Mucha J, Zwiehoff G (1980) Built in test for complex digital integrated circuits. *IEEE J. of Solid State Circuits*, SC 15(3) 315-319.
- 31- Kotorman L (1980) Non charging electron beam pulse prober on FET wafers. *Scanning Electron Microsc.* 1980; IV ; 77-84.
- 32- Lee GH (1946), A three beam microscillograph for recording at frequencies up to 10 000 MC/S. *Proceedings IRE* 34, 121-127.
- 33- Lischke B, Plies B, Schmitt R (1973) Resolution limits in stroboscopic electron beam instruments. *Scanning Electron Microsc.* 1973 : 1177-1185.
- 34- Lukianoff GV, Touw TR (1975) Voltage coding : temporal versus spatial frequencies. *Scanning Electron Microsc.*, 1975 : 465-471.
- 35- Lukianoff GV, Langner GO (1983) Electron beam induced voltage and injected charge modes of testing. *Scanning* 5, 53-70.
- 36- Menzel E (1979) Electron beam chopping systems in the SEM. *Scanning Electron Microsc.* 1979 ; I : 305-318.
- 37- Menzel E, Kubalek E (1981) Electron beam test techniques for integrated circuits. *Scanning Electron Microsc.* 1981 ; I : 305-322.
- 38- Menzel E, Kubalek E (1983) Fundamentals of electron beam testing of integrated circuits. *Scanning Vol. 5*, 103-112.
- 39- Menzel E, Buchanan R (1985) In the lens secondary electron analyser for IC internal voltage measurements with electron beam. *Electronics Letters* 20-10, 408-409.
- 40- Miyoshi M, Ishikawa M, Okumura K (1982) Effects of electron beam testing on the short channel metal oxide semiconductor characteristics. *Scanning Electron Microsc.* 1982; IV: 1507-1514.
- 41- Nakamae K, Fujioka H, Ura K (1981) Local field effects on voltage contrast in the scanning electron microscope. *J. Phys. D : Appl. Phys.*, 14, 1939-1960.
- 42- Nakamae K, Fujioka H, Ura K (1981) Measurements of deep penetration of low energy electrons into metal oxide semiconductor structure. *Journal of Applied Physics* 52 (3) March 1306-1308.
- 43- Oatley CW (1969) Isolation of potential contrast in the scanning electron microscope. *J. of Sci. Instr. (J. of Phys. E) Series 2*, 2, 742-744.
- 44- Plows GS, Nixon WC (1968) Stroboscopic scanning electron microscopy. *J. of Scientific Inst. (J. of Phys. E) Series 2*, 1, 595-600.
- 45- Ranasinghe D, Proctor G, Richardson N (1981) Failure analysis on custom LSI using a modified scanning electron microscope to display voltage waveforms. *Proceedings of Microcircuit Engineering Lausanne*, 1981, 1030-1038.
- 46- Shaver DC (1981) Techniques for electron beam testing and restructuring integrated circuits. *J. Vac. Sc. and Techn.* 19 (4), 1010-1013.
- 47- Singer PH (1986) E-beam probing with CAD interface. *Semicond. International*, Oct. 1986, 26.
- 48- Tamama T, Kuji N (1986) Integrating an electron beam system into VLSI fault diagnosis. *Design and test of computers*, August 1986, 23-29.
- 49- Taylor DM (1978) The effect of passivation on the observation of voltage contrast in the scanning electron microscope. *Journal of Physics*

D: Appl. Phys. 11, 2443-2454.

50- Theus U (1984) Elektronen strahlgesteuerter Wollscheiben. Selbsttest für hoch integrierte digital schaltungen. Thesis Aachen University, 1984.

51- Ura K, Fujioka H, Hosokawa T (1978) Electron optical design of picosecond pulse stroboscopic SEM Scanning Electron Microsc. 1978; I: 747-753.

52- Watanabe, Fukida Y, Jinno T (1985) Analysis of capacitive coupling voltage contrast in scanning electron microscopy. Jap. J. Appl. Phys. 24, 10, 1294-1297.

53- Wells OC (1974) Scanning Electron Microscopy, Mc Graw Hill, New York.

54- Whetten NR (1961) General Electric Lab Report n° Q-RL-2733E Schenectady, New York.

55- Wolfgang E, Lindner R, Fazekas P, Feuerbaum HP (1979) Electron beam testing of VLSI circuits. IEEE Trans. on El. Dev., Vol ED 26, E, 549-559.

#### Discussion with reviewers

A. Gopinath : It is not clear how you arrive at the conclusion that the spatial resolution remains a satisfactory compromise with the blanker and analyzer ? How do you expect it to vary as pulse width reduces, and what do you think this will be at 100 ps ?

Author : The spot size degradation introduced by the blanker is generally reduced with the microscope stigmators. If we assume supplementary degradations due to the analyzer, a satisfactory compromise needs to be found for microscope settings.

I have no special experience of blankers operating with resolutions lower than 100 ps. However, it seems reasonable to expect a spot size increase of 2 between e.g. 1 and 0.1 ns.

J. Beall : What are the primary instrument improvements needed to keep pace with decreasing feature sizes and increasing circuit speeds ? Are there any instrument parameters that will prohibit the future application of SEM QVC ?

Author : One of the important problem connected to E-beam testing seems to be the reduction of the voltage resolution sensitivity to the direction of secondary electrons emission. Both topography and microfield effects are included. It must also be kept in mind the fact that to day remedies are prohibited, say high extraction fields, in the case of CCVC. Since global circuit examinations are required a large field of view is necessary.

Besides, both qualitative and quantitative methods are related to the spot size dimensions. Nowadays with 1 keV, 1 nA at less than 0.1  $\mu\text{m}$  size is always a challenge. According to Fujioka's theoretical work (13), the electron transit time effect introduces some limitations on time resolution.

J. Beall : Have you evaluated radiation hardened MOS devices and their relative sensitivity to SEM QVC ?

Author: Up to now I have not especially worked on radiation hardened MOS devices.

J.Beall: Do you foresee the necessity to decrease beam voltages below 1.0 keV in order to reduce irradiation damage in 1.25 and 0.5 micron device technologies ?

Author : On the one hand, when reducing dimensions, there are no physical reasons against the sensitivity increases to E-beam irradiations. One may think about short channel effects, technology dispersions, etc. Data reported in the literature go in this direction (40). On the other hand a decrease from 1 to 0.5 keV also decreases the magnitude of the threshold shifts between one and two orders of magnitude. This fact needs also to be considered if the logical levels are reduced lower than 5 volts.

W.Reiners : Did you observe a saturation of the threshold voltage shift using a primary electron energy of 6 keV?

Author : Yes, a tendency towards saturation has been observed at this primary energy.